Atom-at-a-time resonance ionization spectroscopy of nobelium

Mustapha Laatiaoui[1,2], Werner Lauth[3], Hartmut Backe[3], Michael Block[1,2,4], Dieter Ackermann[2]†, Bradley Cheal[5], Premaditya Chhetri[6], Christoph Emanuel Düllmann[1,2,4], Piet Van Duppen[7], Julia Even[1]†, Rafael Ferrer[7], Francesca Giacoppo[1,2], Stefan Götz[2,4], Fritz Peter Heßberger[1,2], Mark Huyse[7], Oliver Kaleja[2,8], Jadambaa Khuyagbaatar[1,2], Peter Kunz[9], Felix Lautenschläger[6], Andrew Kishor Mistry[1,2], Sebastian Raeder[1,2,7], Enrique Minaya Ramirez[1]†, Thomas Walther[6], Calvin Wraith[5] & Alexander Yakushev[2]

Experimental study of atomic spectra traditionally required optical spectroscopy of a primordial isotope for each element, providing a benchmark in understanding the atomic structure and revealing how relativistic effects increasingly impact the binding energy of orbital electrons of the heaviest elements. Such studies have been conducted for most elements[1] and theoretical modelling can be performed to high precision[2,3]. Today, no tabulated spectral lines exist for the transfermium elements of an atomic number Z>100. These radioactive elements are produced in nuclear fusion reactions at rates of a few atoms per second at most and must be studied 'live' immediately following their production, which so far precluded their optical spectroscopy. Here, we report on radioactive decay-detected resonance ionization spectroscopy on the element nobelium (No), the 102nd element in the periodic table, in which we identified the ground-state transition $^1S_0 \rightarrow {}^1P_1$. Combined with data from an observed Rydberg series, an upper-limit for the ionization potential (IP) is obtained. These accurate results provide a particular challenge for state-of-the-art relativistic many-body calculations[5,6,7,8] addressing quantum electrodynamic effects. The present work opens the door for high-precision measurements of various atomic and nuclear properties also of elements heavier than nobelium and motivates future theoretical work.

Since the establishment of the actinide elements in the periodic table, great efforts have been undertaken to investigate their atomic spectra[9]. The prevailing strategy included deducing many of the atomic properties from a detailed knowledge of the electronic configuration, which is subject to strong relativistic effects. This approach was driving large optical spectroscopy research programs for many years, which yielded detailed insight into the atomic structure of elements up to einsteinium[1] including precise values for their IP. The heaviest element for which optical spectroscopy has hitherto been reported is fermium with Z = 100 (ref. 10). A sample of about 10 pg of ^{255}Fm with a half-life of $T_{1/2}$ = 20.1 h facilitated resonance laser ionization spectroscopy experiments[11,12]. The transfermium elements, in contrast, neither occur naturally on earth nor can macroscopic samples be synthesized. These elements are typically produced at large accelerator facilities by heavy-ion induced fusion-evaporation reactions, which only yield low rates. Some of their atomic properties had been accessible in aqueous-phase and gas-phase chemical studies[13,14]. Only recently, the first ionization potential was experimentally determined for lawrencium (Z = 103, Lr) applying surface ionization techniques[15].

Advancing optical studies to the region of the transfermium elements calls for fast spectroscopy techniques of extreme sensitivity[4]. Challenges in this research field include producing such atoms, separating them from undesired species, which are inevitably co-produced, manipulating and detecting them within seconds, to mention but a few. In our experiments we applied a RAdiation Detected Resonance Ionization Spectroscopy (RADRIS) technique[16,17], using a two-step photoionization process[18] for ionizing nobelium atoms (Z = 102). Similar techniques had previously been employed for laser spectroscopy of short-lived americium fission isomers at production rates as low as ten per second[19,20]. For such an approach to become feasible for elements like nobelium, requires an extensive search for atomic transitions within a spectral range proposed by state-of-the-art model calculations. Unambiguous identification of the atoms is achieved via their unique radioactive decay fingerprint[21].

The isotope ^{254}No with a half-life $T_{1/2}$ = 51.2 s was chosen for the first laser spectroscopy experiments. This isotope was produced in the two-neutron evaporation channel of the complete-fusion reaction ^{48}Ca+^{208}Pb. The fusion products, emerging from a thin ^{208}Pb target, were separated in-flight from the intense ^{48}Ca primary beam by the Separator for Heavy Ion reaction Products (SHIP)[22] at the GSI Helmholtzzentrum für Schwerionenforschung. About four ^{254}No ions per second were implanted in a buffer-gas stopping cell installed in the SHIP's focal plane[4]. They were thermalized in 95 mbar high-purity argon gas and accumulated and neutralized on a tantalum catcher filament (see

[1]Helmholtz-Institut Mainz, Johann-Joachim-Becher Weg 36, D-55128 Mainz, Germany. [2] GSI Helmholtzzentrum für Schwerionenforschung GmbH, Planckstr. 1, D-64291 Darmstadt, Germany. [3] Institut für Kernphysik, Johannes Gutenberg-Universität, Johann-Joachim-Becher-Weg 45, D-55128 Mainz, Germany. [4] Institut für Kernchemie, Johannes Gutenberg-Universität, Fritz-Strassmann-Weg 2, D-55128 Mainz, Germany. [5] Department of Physics, University of Liverpool, Oxford Street, L69 7ZE Liverpool, UK. [6] Institut für Angewandte Physik, Technische Universität Darmstadt, Schlossgartenstr. 7, D-64289 Darmstadt, Germany. [7] Instituut voor Kern- en Stralingsfysica, KU Leuven, Celestijnenlaan 200D, B-3001 Leuven, Belgium. [8] Institut für Kernphysik, Technische Universität Darmstadt, Schlossgartenstr. 9, D-64289 Darmstadt, Germany. [9] TRIUMF, 4004 Wesbrook Mall, Vancouver BC V6T 2A3, Canada. †Present addresses: Grand Accélérateur National d'Ions Lourds, Bd Henri Becquerel, BP 55027 - 14076 Caen Cedex 05, France (D.A.); KVI - Center for Advanced Radiation Technology, Rijksuniversiteit Groningen, Zernikelaan 25, 9747 AA Groningen, Netherlands (J.E.); Institut de Physique Nucléaire Orsay, 15 rue Georges Clémenceau, 91406 Orsay, France (E.M.R)

Methods section). For a short time during every measurement cycle, the incoming flux of ^{254}No ions was turned off and the adsorbed nobelium atoms were evaporated from the filament by heating this briefly to a temperature of about 1,350 K. Nobelium atoms in the ground state $5f^{14}7s^2\,{}^1S_0$ residing in laser beam paths in the vicinity of the filament will undergo element-selective ionization in a two-step excitation scheme as shown in the inset of Fig. 1a. The ionization proceeded by resonantly exciting the singlet state $5f^{14}7s7p\,{}^1P_1$ with ultraviolet (UV) light from a tunable dye laser (λ_1), followed by a second excitation into the continuum beyond the IP with UV light in the wavelength range 349-353 nm (λ_2) from a more powerful excimer laser. Induced photoions are subsequently guided by electrostatic fields to a silicon detector where the characteristic alpha decay of ^{254}No is detected[23].

A spectral range from 28,887 to 33,191 cm^{-1} was chosen to locate the $^1S_0 \rightarrow {}^1P_1$ atomic transition in nobelium (Methods). Latest predictions based on Multi-Configuration-Dirac-Fock (MCDF) and Relativistic-Coupled-Cluster calculations[5,6,7,8] suggest wavenumber values clustering between 29,256 and 31,709 cm^{-1} (Table 1a) for the excited state $^1P_1$. The sufficient treatment of correlation effects by the different approaches decisively improved the picture given by the first MCDF calculations[24] focusing on quantum electrodynamic effects. Nonetheless, about 6,110 laser scan steps needed to be conducted before discovering this elusive first-step resonance. In Fig. 1a (full triangles) we show the observed resonance in terms of normalized alpha-decay count rates. A relatively high laser power was initially used, which was favorable for an efficient level search leading to a power-broadened transition. It is centered at a wavenumber of $\bar{\nu}_1' = 29,961.457^{+0.041}_{-0.007}$ cm^{-1} as determined from a subsequent narrowband scan using an intra-cavity etalon, see Fig. 1a (bullets). The dominant part in the quoted uncertainties originates from the pressure shift (Extended Data Table 1) resulting in a 1.4-parts-per-million relative precision, which is far more precise than from modern theories, and hence provides a powerful benchmark. Table 1a gives a comparison of the experimental result for the wavenumber of the $^1P_1$ state with theoretical predictions.

Having located the resonance in ^{254}No the spectral resolution was increased in order to measure the isotope dependence of the $^1S_0 \rightarrow {}^1P_1$ transition energy by reducing the laser intensity. In Fig. 1b we show the measurement on the same transition in ^{252}No ($T_{1/2}$ = 2.4 s), produced under similar conditions using a ^{206}Pb target. Successful spectroscopy was achieved with implantation rates lower than one atom per second delivered to the buffer-gas stopping cell indicating the high efficiency of our setup (Methods). We observed a signal displacement, the isotope shift, of about 0.32 cm^{-1}, which is due to a difference in nuclear size and shape and will be published in a separate paper focussing on the nuclear structure aspects of our work.

To further confirm the identification of the $^1P_1$ state, the saturation characteristics of the first-step resonance has been measured (Fig. 2). Saturation was observed at rather low photon fluxes, which is a clear indication for a sizable dipole-transition amplitude. We obtained a corresponding Einstein coefficient for spontaneous emission of $A_{ki} = 4.2^{+2.6}_{-2.8} \times 10^8\,\mathrm{s}^{-1}$ by fitting a rate-equation model (P.C., H.B. et al., manuscript in preparation) to the saturation data. This value is in agreement with various theoretical predictions (Table 1a) supporting that the short-lived $5f^{14}7s7p\,{}^1P_1$ atomic state was observed.

We also observed several high-lying Rydberg states in ^{254}No (Fig. 3a-c). The first excitation step was set to the resonance at $\bar{\nu}_1' = 29,961.457\,\mathrm{cm}^{-1}$, while the second step was scanned with a dye laser in the range from 23,460 cm^{-1} to 23,503 cm^{-1}. Two pronounced peaks, potentially members of the same Rydberg series, were observed. Sampling in an extended scan range revealed further peaks belonging to the same series, which so far could not be assigned unambiguously.

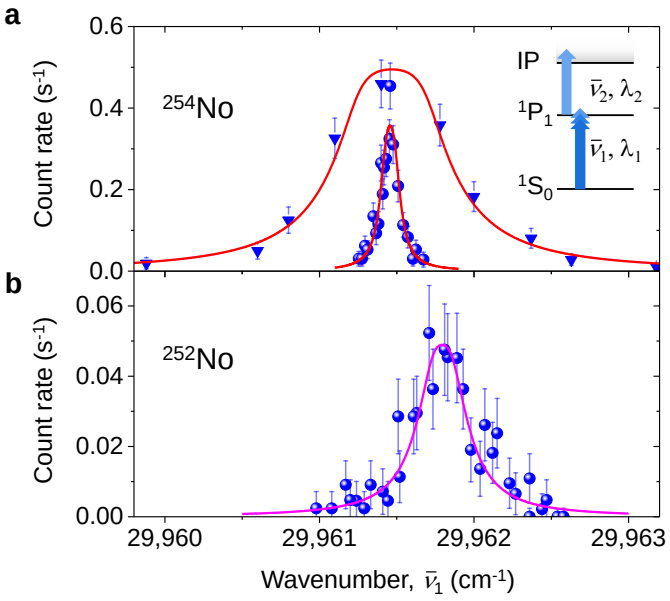

Figure 1: For caption see end of main text.

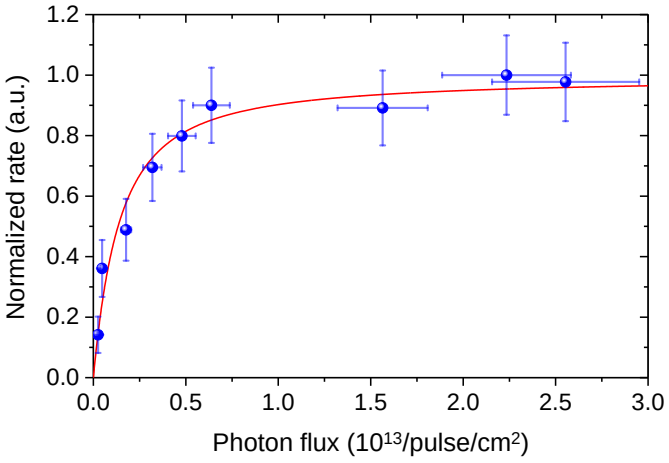

Figure 2: For caption see end of main text.

Table 1: For caption see end of main text.

a Atomic state $5f^{14}7s7p\,^1\mathrm{P}_1$ in ^{254}No		
Method	$\overline{\nu}_1'$ (cm^{-1})	A_{ki} (s^{-1}) $\times 10^8$
Experiment	$29,961.457^{+0.041}_{-0.007}$	$4.2^{+2.6}_{-2.8}$
CI+all-order [8] ♯	$30,203 \pm 600$	
MCDF [7] ♭	$30,609 \pm 1100$ *	3.5
IHFSCC [6] §	$30,056 \pm 800$	5.0
MCDF [5] ♭	$30,650 \pm 800$	2.7
b Ionization potential		
Method	IP (cm^{-1})	
Experiment	$52,467$ ** $\leq$IP$\leq 53,757.5$	
CI+all-order [8] ♯	$54,390 \pm 1100$	
MCDF [7] ♭	$53,701 \pm 1100$ ***	
IHFSCC [6] §	$53,489 \pm 800$ ***	
Extrapolation [25]	$53,600 \pm 600$	

♯ Configuration interaction method combined with the linearized single-double coupled cluster method (all-order).
♭ Multi-configuration Dirac-Fock.
§ Intermediate Hamiltonian Fock-space coupled cluster.
* As not explicitly reported in the original paper, we assessed the error from the relative difference of the calculated and measured values for the corresponding state in ytterbium.
** The lower limit of the IP has been estimated from theoretical calculations [6], for details see text.
*** We give a conservative error, the magnitude of which is based on that of the error of the $^1\mathrm{P}_1$ state wavenumber evaluated with the corresponding method (Table 1a).

In the absence of perturbations originating from the interaction with buffer gas atoms, the transition energies from the excited $^1\mathrm{P}_1$ state to Rydberg states $h\nu_2(n)$ follow a trend described by the well-known Rydberg formula [18] $h\nu_2(n) = h\nu_{lim} - R_m/(n-\delta)^2$. Here, $h\nu_{lim} = \mathrm{IP} - h\nu_1'$ denotes the ionization limit for the excited state, n, the principal quantum number of the valence electron, R_m, the reduced-mass Rydberg constant for ^{254}No, and δ, the quantum defect. In the first-order Ritz expansion [26] the quantum defect can be expressed as $\delta(n) = \delta_0 + B/(n-\delta_0)^2$ with the fitting parameters δ_0 and B. In the upper panel of Fig. 3d, the positions of the observed peaks are plotted against their principal quantum number n. The n assignment was based on restricting the quantum defect to be in the range between 0 and 1, i.e., arbitrary, as the outcome of the analysis remained unaffected by this choice. The best fit to the data showed a convergence towards the value $\overline{\nu}_{lim} = 23,785^{+11}_{-1}\,\mathrm{cm}^{-1}$. From higher-order corrections in the quantum defect, we estimated a maximum systematic error of $+10\,\mathrm{cm}^{-1}$ for the given value. Shifts in the atomic spectra due to the buffer gas pressure were neglected as these are expected not to exceed $0.5\,\mathrm{cm}^{-1}$. However, experimental observations when delaying the non-resonant ionizing laser pulse, suggest a fast quenching of the $^1\mathrm{P}_1$ state, induced by buffer-gas collisions, into a potentially long-lived but energetically very close atomic state. Hence, the observed series is not necessarily excited from the $^1\mathrm{P}_1$ state. Possible candidates are a $^3\mathrm{D}_3$ or even a $^3\mathrm{D}_2$ state, located $159\,\mathrm{cm}^{-1}$ and $1,278\,\mathrm{cm}^{-1}$ below the $^1\mathrm{P}_1$ state according to ref. 6, respectively. We thus include a lower limit for the ionization potential of nobelium as $\overline{\nu}_{lim} + \overline{\nu}_1' - 1,278\,\mathrm{cm}^{-1} = 52,467\,\mathrm{cm}^{-1}$ corresponding to 6.505 eV. The upper limit is $\overline{\nu}_{lim} + \overline{\nu}_1' = 53,757.5\,\mathrm{cm}^{-1}$ (6.665 eV). This is because any populated state energetically lying above the $^1\mathrm{P}_1$ state would immediately depopulate to the then lower-lying $^1\mathrm{P}_1$ and cannot lead in this context to delayed resonance ionization. In Table 1b various theoretical predictions are compared with our experimental value for the IP. This value continues the trend of increasing IP along the heaviest actinides [1,27] and is significantly higher than the one recently reported for the heavier element lawrencium [15]. In analogy to the lanthanides, the lighter homologues, this corroborates the scenario of closed $5f$ and $7s$ atomic-shells in nobelium.

In summary, laser spectroscopy of the element nobelium was successfully performed using the ultra-sensitive and highly efficient RADRIS technique. This marks a basis for future experiments, in which atomic-level energies of nobelium including the first IP can be determined with unprecedented precision. The new data provide anchor points for future theoretical work, which in turn forms an indispensable guide for such experiments. This work opens up a new horizon for laser spectroscopy in the elusive region of the heaviest elements, including those beyond nobelium, accessible with even lower yield, with different atomic structure. An example is the heaviest actinide element lawrencium, which is now within reach of such studies. Moreover, isotope shift and hyperfine structure measurements [28] on nobelium isotopes are now feasible, forming a valuable contribution to nuclear structure studies in the region of deformed nuclei on the shore of the 'superheavy elements', elements which only exist due to nuclear shell structure. These sophisticated alternatives to established in-beam and decay spectroscopy approaches [29] provide complementary information on both single-particle and collective properties, alongside spin assignments, and will critically test and revise state-of-the-art nuclear models.

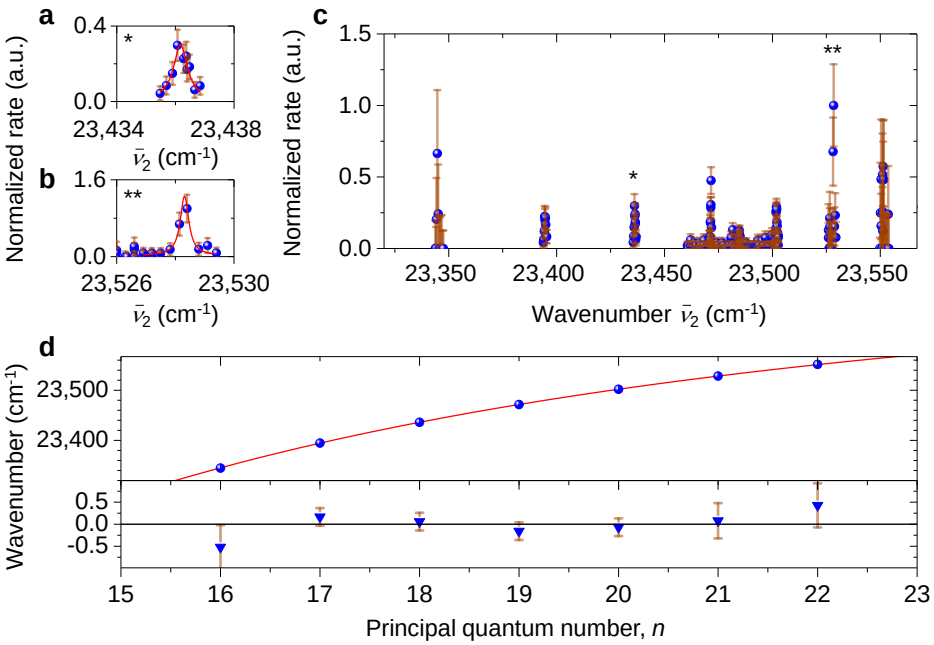

Figure 3: For caption see end of main text.

1. Kramida, A., Ralchenko, Y., Reader, J. & NIST-Team. *NIST Atomic Spectra Database* version 5.3 (2016); http://physics.nist.gov/asd (accessed March 2016).
2. Eliav, E., Fritzsche, S. & Kaldor, U. Electronic structure theory of the superheavy elements. *Nucl. Phys. A* **944** 518-550 (2015).
3. Schwerdtfeger, P., Pašteka, L.F., Punnett, A. & Bowman, P.O. Relativistic and quantum electrodynamic effects in superheavy elements. *Nucl. Phys. A* **944** 551-577 (2015).
4. Backe, H., Lauth, W., Block, M. & Laatiaoui, M. Prospects for laser spectroscopy, ion chemistry and mobility measurements of superheavy elements in buffer-gas traps. *Nucl. Phys. A* **944** 492-517 (2015).
5. Indelicato, P., Santos, J.P., Boucard, S. & Desclaux, J.-P. QED and relativistic corrections in superheavy elements. *Eur. Phys. J. D* **45**, 155-170 (2007).
6. Borschevsky, A. et al. Predicted spectrum of atomic nobelium. *Phys. Rev. A* **75**, 042514 (2007).
7. Liu, Y., Hutton, R. & Zou, Y. Atomic structure of the superheavy element No I (Z = 102). *Phys. Rev. A* **76**, 062503 (2007).
8. Dzuba, V.A., Safronova, M.S. & Safronova, U.I. Atomic properties of superheavy elements No, Lr, and Rf. *Phys. Rev. A* **90**, 012504 (2014).
9. Worden, E.F, Blaise, J., Fred, M., Trautmann, N. & Wyart, J.-F. Spectra and Electronic Structures of Free Actinide Atoms and Ions. In *The Chemistry of the Actinide and Trans-actinide Elements* (eds Morss, L.R., Edelstein, M., Fuger, J.) vol. 3, Ch. 16.4 (Springer, 2008).
10. Sewtz, M. et al. First Observation of Atomic Levels for the Element Fermium (Z = 100). *Phys. Rev. Lett.* **90**, 163002 (2003).
11. Sewtz, M. et al. Resonance ionization spectroscopy of fermium (Z = 100). *Spectrochim. Acta B* **58**, 1077-1082 (2003).
12. Backe, H. et al. Laser Spectroscopic Investigation of the Element Fermium (Z = 100). *Hyperfine Interact.* **162**, 3-14 (2005).
13. Nagame, Y., Kratz, J.V. & Schädel, M. Chemical studies of elements with Z≥104 in liquid phase. *Nucl. Phys. A* **944** 614-639 (2015).
14. Türler, A., Eichler, R. & Yakushev, A. Chemical studies of elements with Z≥104 in gas phase. *Nucl. Phys. A* **944** 640-689 (2015).
15. Sato, T.K. et al. Measurement of the first ionization potential of lawrencium, element 103. *Nature* **520**, 209-211 (2015).
16. Lauth, W. et al. Resonance Ionization Spectroscopy in a Buffer Gas Cell with Radioactive Decay Detection, Demonstrated Using ^{208}Tl. *Phys. Rev. Lett.* **68**, 1675-1678 (1992).
17. Backe, H. et al. Towards optical spectroscopy of the element nobelium (Z = 102) in a buffer gas cell. *Eur. Phys. J. D* **45**, 99-106 (2007).
18. Letokhov, V.S. *Laser Photoionization Spectroscopy* (Academic Press, 1987).
19. Backe, H. et al. Isotope Shift Measurements for Superdeformed Fission Isomeric States. *Phys. Rev. Lett.* **80**, 920-923 (1998).
20. Backe, H. et al. Stability of Superdeformation for Americium Fission Isomers as Function of the Neutron Number. *Nucl. Phys. A* **690**, 215c-218c (2001).
21. Laatiaoui, M. et al. On laser spectroscopy of the element nobelium (Z = 102). *Eur. Phys. J. D* **68**, 71-77 (2014).
22. Hofmann, S. & Münzenberg, G. Discovery of the heaviest elements. *Rev. Mod. Phys.* **72**, 733-767 (2000).
23. Lautenschläger, F. et al. Laser spectroscopy of the heaviest elements at SHIPTRAP. *Nucl. Instrum. Methods B* (2016), accepted.
24. Fritzsche, S. On the accuracy of valence-shell computations for heavy and super-heavy elements. *Eur. Phys. J. D* **33**, 15-21 (2005).
25. Sugar, J. Revised ionization energies of the neutral actinides. *J. Chem. Phys.* **60**, 4103 (1974).
26. Martin, W.C. Series formulas for the spectrum of atomic sodium (Na I). *J. Opt. Soc. Am.* **70**, 784-788 (1980).
27. Wendt, K., Gottwald, T., Mattolat, C. & Raeder, S. Ionization potentials of the lanthanides and actinides - towards atomic spectroscopy of super-heavy elements. *Hyperfine Interact.* **227**, 55-67 (2014).
28. Campbell, P., Moore, I.D. & Pearson, M.R. Laser spectroscopy for nuclear structure physics. *Prog. Part. Nucl. Phys.* **86**, 127-180 (2016).

29. Herzberg, R.-D. et al. Nuclear isomers in superheavy elements as stepping stones towards the island of stability. *Nature* **442**, 896-899 (2006).

Supplementary Information is available in the online version of the paper.

Acknowledgements We thank the staff of the GSI ion source and accelerator for the preparation of stable ^{48}Ca beam as we are grateful to the staff of the target lab for providing high-quality targets. We acknowledge the technical support of J. Maurer, H.G. Burkhard, D. Racano, L. Braisz, D. Reemts, C. Droese, B. Schausten and I. Kostyuk. We thank P. Thirolf for his suggestions and comments. This work was supported by the German Federal Ministry of Research under contracts 06MZ169I, 06LM236I, FAIR NuSTAR 05P09RDFN4, 05P12RDFN8, and 05P15RDFN1; by the GSI; and by the Helmholtz-Institut Mainz.

Author Contributions W.L., H.B., M.B., T.W., P.v.D., C.E.D., M.H. and A.Y. provided experimental equipment. M.L., F.L., P.C., S.R., W.L., P.K., M.B., F.P.H., D.A., C.W., A.K.M., B.C., R.F., F.G., O.K., J.K., J.E., S.G., and E.M.R. performed the experiments. F.L., P.C., H.B., S.R. and M.L. analyzed the data. M.L. wrote the manuscript with input from all authors.

Author Information Reprints and permissions information is available at www.nature.com/reprints. The authors declare no competing financial interests. Readers are welcome to comment on the online version of the paper. Correspondence and requests for materials should be addressed to M.L.(M.Laatiaoui@gsi.de).

Figure 1: **Resonance ionization signals of nobelium atoms. a**, Scans over the first-step resonance in ^{254}No. The count rates are normalized to a beam current of one particle microampere, equivalent to 6.2×10^{12} ^{48}Ca projectiles per second. Best fits to the data on the basis of a rate-equation model are indicated by solid lines. Full triangles: $0.80\,\mathrm{cm}^{-1}$ fit profile full width at half-maximum (FWHM); photon flux: 1.1×10^{14} photons/pulse/cm^2; laser bandwidth: $0.18\,\mathrm{cm}^{-1}$; bullets: $0.13\,\mathrm{cm}^{-1}$ fit profile FWHM; photon flux: 5.2×10^{12} photons/pulse/cm^2; laser bandwidth: $0.04\,\mathrm{cm}^{-1}$. Inset: a simplified ionization scheme. **b**, Same as **a**, but for ^{252}No. $0.36\,\mathrm{cm}^{-1}$ fit profile FWHM; photon flux: 1.1×10^{13} photons/pulse/cm^2; laser bandwidth: $0.18\,\mathrm{cm}^{-1}$. Error bars, ±1 s.d.

Figure 2: **Saturation characteristics of the first-step resonance for ^{254}No.** Alpha-decay count rates at the resonance peak, normalized to the maximum value, are displayed versus the photon flux of the first excitation step. Laser bandwidth: $0.18\,\mathrm{cm}^{-1}$. The flux for the second step was kept at 7.3×10^{15} photons/pulse/cm^2 during this measurement. A best-fitting to the data according to a rate-equation model is also shown (solid line). All error bars indicate ±1 s.d.

Table 1: **Experimental and theoretical values for the ^{1}P$_1$ state and the ionization potential of nobelium.**

Figure 3: **Observed high-lying Rydberg states in nobelium. a-c**, ^{254}No alpha-decay count rates, normalized to the maximum value, versus the excitation-energy equivalent wavenumber for the second-step excitation. First-step excitation: $\overline{\nu}_1' = 29,961.457\,\mathrm{cm}^{-1}$. Two selected Rydberg resonances with Lorentzian-profile fits (solid lines) to the data are shown in **a** and **b** and indicated by corresponding asterisks in **c**. **d**, Top panel: the position of 7 high-lying Rydberg states (bullets) as a function of n and a corresponding best fit (solid line) according to the Rydberg-Ritz formula. The residuals of the fit (full triangles) are shown in the bottom panel. Error bars, ±1 s.d.

Extended Data Table 1: **Uncertainties for the value of the ^{254}No first-step resonance.** The peak-position in the narrowband-scan data is extracted from a best fit based on a rate-equation model. The value for the wavelength measurement represents the accuracy of the wavelength meter in multimode-fiber operation. A conservative value for the pressure shift is taken from ref. 16.

Extended Data Figure 1: **Principle of the RADRIS technique.** Laser spectroscopy on radionuclides after their production and transmission through the velocity filter SHIP[22]. a, Thermalization of the fusion products in the buffer gas; b, accumulation on the catcher filament; c, re-evaporation from the filament; d, two-step photoionization of neutral atoms; e, accumulation of re-ionized fusion products on the PIPS detector; f, decay detection.

Methods

Production of ^{252}No and ^{254}No. The experiments described in this paper were carried out behind the velocity filter SHIP [22] at the linear accelerator (UNILAC) of GSI Helmholtzzentrum für Schwerionenforschung in Darmstadt. The isotopes ^{252,254}No were produced in the complete-fusion evaporation reactions ^{206}Pb(^{48}Ca,2n)^{252}No and ^{208}Pb(^{48}Ca,2n)^{254}No at UNILAC beam energies of 217 MeV with cross sections of 515^{+80}_{-47} nb and 2050^{+460}_{-340} nb (ref. 30), using lead sulfide (PbS) targets [31] of 460 μg/cm^2 and 470 μg/cm^2 average thickness, respectively, which remained constant throughout the measurements. The ^{48}Ca^{10+} beam from the UNILAC exhibited a macro-pulse structure of 5 ms beam-on and 15 ms beam-off. Beam currents were typically 0.7 particle microampere (about 4.4×10^{12} particles per second). For laser spectroscopy experiments, the beam was further chopped in accordance with user-defined measurement cycles. In the case of ^{254}No, the implantation rate of the fusion products delivered to the experiment was repeatedly checked by a retractable position-sensitive 16-strip silicon detector placed at the focal plane of SHIP.

Radiation Detected Resonance Ionization Spectroscopy. The fusion-evaporation residues with a mean kinetic energy of about 41 MeV (ref. 23) were separated from the ^{48}Ca primary beam by the velocity filter SHIP and subsequently thermalized inside the optical cell, a buffer-gas stopping cell filled with 95 mbar argon of ultrahigh purity (99.9999%). The cell was separated from the vacuum of the SHIP by a 3.5-μm thick entrance foil (Mylar) on a support grid, see Extended Data Fig. 1. The geometrical transparency of the grid amounts to 90.3%. A substantial fraction of the stopped fusion products remained in a positive charged state and was collected during the accumulation time of every measurement cycle onto a catcher filament, a tantalum wire of 125 μm diameter. The filament was heated for 300 ms to a temperature of about 1,350 K, triggering the evaporation of neutral nobelium atoms for subsequent two-step laser ionization [21]. Ions produced during this process were promptly guided by suitable electric fields to a particle detector, a Passivated Implanted Planar Silicon semiconductor detector (PIPS), with which the characteristic alpha-decay or spontaneous fission of the studied nobelium isotopes and their descendants was registered [17,21,23]. The optimum accumulation time depends on the half-life of the isotope under consideration and was 25 s (ref. 32) in case of ^{254}No with $T_{1/2} = 51.2 \pm 0.4$ s (ref. 29). The two-step laser ionization took place during a 5-s time window every cycle, while the primary ion beam was switched off. Correspondingly, 3-s-beam-on and 3-s-beam-off periods were chosen in the case of the short-lived isotope [33] ^{252}No ($T_{1/2} = 2.42 \pm 0.06$ s). We further introduced 'waiting' cycles by interrupting the data acquisition while changing the laser frequencies. In Fig. 1a, for instance, a 'waiting' cycle of 5 minutes was chosen, necessary especially in the case of ^{254}No, in order to minimize residual ^{254}No alpha-decay events that might lead to counts not belonging to the chosen laser frequency. The absolute temperature of the filament was monitored using a fast infrared pyrometer (LumaSense Inc., IMPAC IS 6 Advanced). The temperature was adjusted to the nominal value when necessary in order to prevent overheating, which was observed to lead to increased background in preparatory experiments.

Laser setup for nobelium spectroscopy. The extended level search in nobelium was carried out using four tunable excimer laser-pumped dye lasers (Lambda Physik, FL and LPD series, bandwidth (5.5 ± 0.5) GHz) and an Optical Parametric Oscillator (OPO) system (GWU-Lasertechnik, VisIR2, bandwidth ≈ 90 GHz) pumped by a frequency-tripled Nd:YAG laser (Continuum, Powerlite DLS 8050). Except for the latter 50-Hz system, all the other pump lasers were operated at a repetition rate of 100 Hz. The laser pulse duration was at most 18 ns (FWHM) with a jitter < 11 ns for all of them. The dye lasers were set up to scan in the range from 25,000 cm^{-1} up to 31,000 cm^{-1}. During the level search in nobelium, however, the scans were conducted mainly in the UV region of the optical spectrum. With a mean step size of about 0.89 cm^{-1} we thereby covered more than twice the spectral range from 28,887 cm^{-1} to 30,530 cm^{-1}. With the OPO system, operated in a frequency-mixing mode, and by choosing a scan step size of 3 cm^{-1}, adapted to the laser bandwidth, multiple scans from 30,000 up to 33,191 cm^{-1} were conducted. The laser wavelengths were continuously monitored with a wavelength meter (HighFinesse-Ångstrom, WS/7-UVU) that was calibrated to an internal neon lamp. Laser pulse energies in excess of 0.1 mJ were repeatedly measured at the optical cell for all tunable lasers. For an efficient beam time usage they were operated simultaneously in different wavelength ranges. They were synchronized with excimer laser synchronization units (Lambda Physik, LPA 97) with respect to the ionizing laser, an excimer laser (Lambda Physik, LPX220) delivering an average pulse energy of 45 mJ of broadband laser light in the wavelength range 349-353 nm at the optical cell. The total photon energy available for ionization was by far higher than all theoretical predictions and extrapolations of the IP of nobelium (Table 1b). The scans near the IP were performed by replacing the excimer ionizing laser by a tunable dye laser scanning in the blue range of the optical spectrum. Here, only two dye lasers were operated simultaneously. In addition, the dye lasers enabled the use of intra-cavity etalons and thus a narrowing of the laser bandwidth down to 1.2 GHz. The narrow resonance shown in Fig. 1a (bullets) was recorded using this option. More details on the laser systems used can be found in ref. 23.

RADRIS efficiency. The overall efficiency of the setup is defined as the ratio of the nobelium decay count rate measured with the PIPS detector A_{RIS} at maximum of a resonance to the implantation rate of nobelium ions delivered to the optical cell A_{Ion}, both normalized to the intensity of the primary beam. The spatial distribution of the ^{254}No ions delivered to the experiment was best described by a 2D-Gaussian distribution with $\sigma_x = 22$ mm and $\sigma_y = 5.7$ mm based on a measurement with the position-sensitive 16-strip silicon detector exhibiting an active area of 80 mm $\times$ 35 mm. The ion implantation rate was extracted from the alpha-decay count rate A_α measured with this detector according to $A_{Ion} = A_\alpha/(\varepsilon_\alpha \times \varepsilon_\Omega \times \varepsilon_{daq})$, with $\varepsilon_\alpha = 0.9$, the alpha-decay probability for ^{254}No, $\varepsilon_\Omega = 0.55$, the solid angle coverage for alpha decays from implanted ^{254}No recoils [23], and $\varepsilon_{daq} = 0.77$, the efficiency for data acquisition, which was limited to the beam-off time windows during which data recording occurred. On average, decay rates in the PIPS detector of 0.39 ± 0.05 and 0.048 ± 0.006 per second and particle microampere (6.2×10^{12} ^{48}Ca projectiles per second) were obtained for ^{254}No and ^{252}No, respectively. With these numbers an overall efficiency of the apparatus of (6.4 ± 1)% and (3.3 ± 1)% was calculated, respectively, proving a high-efficiency of the applied spectroscopy technique. The difference in the quoted numbers is mainly due to the half-lives of the isotopes under investigation. In the spectroscopy of ^{252}No a shortest possible beam-off period of 3 s was applied. Even though the measurement cycle was optimized to minimize the impact of the half-life on the overall efficiency, the spectroscopy of ^{252}No turned out to be less efficient compared with ^{254}No.

30. Oganessian, Yu.Ts. et al. Measurements of cross sections for the fusion-evaporation reactions ^{204,206,207,208}Pb+^{48}Ca and ^{207}Pb+^{34}S: Decay properties of the even-even nuclides ^{238}Cf and ^{250}No. *Phys. Rev. C* **64**, 054606 (2001).
31. Kindler, B. et al. Chemical compound targets for SHIP on heated carbon backings. *NIMA* **561**, 107-111 (2006).
32. Laatiaoui, M. et al. Perspectives for laser spectroscopy of the element nobelium. *Hyperfine Interact.* **227**, 69-75 (2014).
33. Sulignano, B. et al. Identification of a K isomer in ^{252}No. *Eur. Phys. J. A* **33**, 327-331 (2007).

Extended Data Table 1: For caption see end of main text.

Origin	Uncertainty (cm^{-1}) $\times 10^{-3}$
Fit	± 4.2
Wavelength measurements	± 5.0
Pressure shift	$+34.2$

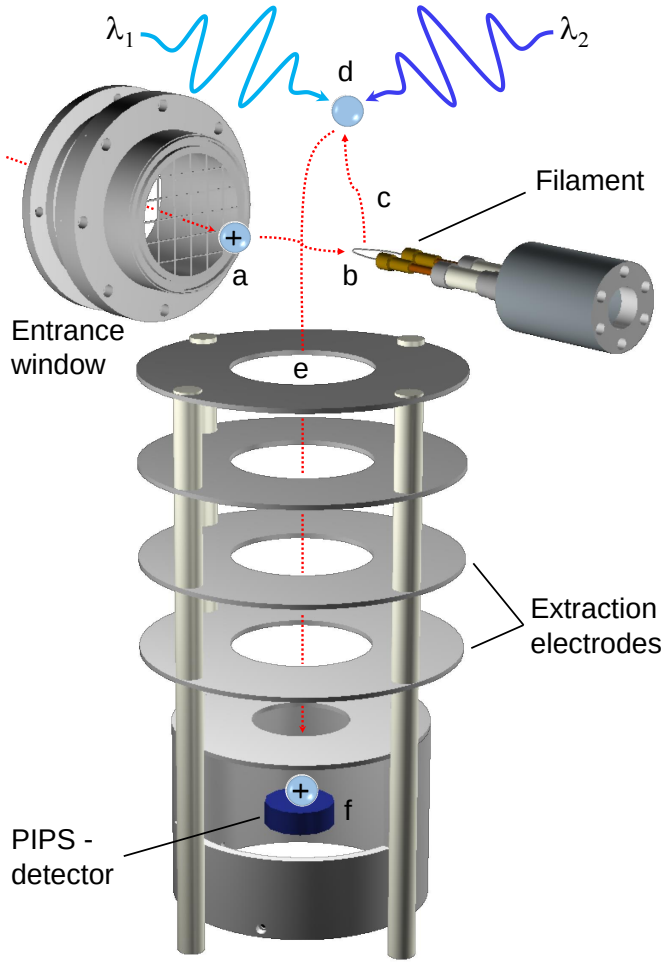

Extended Data Figure 1: For caption see end of main text.